

An Alternating Direction Implicit Scheme for Parabolic Equations with Mixed Derivative and Convective Terms

S. MCKEE, D. P. WALL, AND S. K. WILSON

Department of Mathematics, University of Strathclyde, Livingstone Tower, 26, Richmond Street, Glasgow, G1 1XH, United Kingdom

Received February 2, 1994; revised April 24, 1995

THIS PAPER IS DEDICATED TO PROFESSOR A. R. MITCHELL ON THE EVENT OF HIS 75TH BIRTHDAY

An alternating direction implicit (ADI) scheme is introduced which is capable of solving a general parabolic equation in two space dimensions with mixed derivative and convective terms. In the case of constant coefficients the scheme is shown to be unconditionally stable. The study was motivated by the investigation of flow in a dye laser cell (a device used for the amplification of a laser beam), a simple model for which involves laminar flow in a two-dimensional symmetric channel subject to impulsive heating. Numerical results are presented for this problem, and the qualitative behaviour of the temperature distribution within the channel for different Peclet numbers is discussed. © 1996 Academic Press, Inc.

1. INTRODUCTION

The purpose of this paper is to introduce an unconditionally stable ADI scheme capable of solving the general parabolic partial differential equation

$$\frac{\partial T}{\partial t} + u \frac{\partial T}{\partial x} + v \frac{\partial T}{\partial y} = a \frac{\partial^2 T}{\partial x^2} + b \frac{\partial^2 T}{\partial x \partial y} + c \frac{\partial^2 T}{\partial y^2}, \quad (1.1)$$

where the functions $a, c, u, v > 0$, and $b^2 < 4ac$. The development of such a scheme was motivated by the physical problem of heated fluid flow through a dye laser cell outlined in Section 2, which requires the solution of the two-dimensional heat-transport equation on a non-rectilinear domain. The use of boundary fitted coordinates allows the problem to be solved on a rectilinear domain but transforms the governing partial differential equation to the more general form given by Eq. (1.1); accordingly an ADI method appropriate for the solution of Eq. (1.1) is introduced in Section 3 and the scheme's unconditional stability is shown. The extension of the scheme to N dimensions is also discussed. In Section 4 the scheme is applied to the dye laser cell problem and results are presented for a variety of different values of the Peclet number which represents the balance between convection and diffusion terms. Some concluding remarks are offered in Section 5.

2. PHYSICAL BACKGROUND AND MOTIVATION

2.1. Problem Formulation

A dye laser cell is a device which amplifies a highly tuned laser beam via an energy transfer from a second, untuned, but more powerful laser beam. Fluorescent dye is passed at high speed through a narrow convergent/divergent channel and impulsively heated at the neck. For further details see Duarte and Hillman [6] or Schäfer [13].

A first step in modelling the heat and mass transfer of the fluid in the dye laser cell may be achieved by considering the convection/diffusion equation together with a lubrication approximation for the fluid flow. (For such an approximation to be valid we require the flow in the channel to remain laminar; experimental results suggest that this is the case, but the onset of turbulence is an important and difficult question and is the subject of ongoing research.) This model requires the solution of the non-dimensionalised two dimensional heat-transport equation

$$\frac{\partial T}{\partial t} + \text{Pe} \left(u \frac{\partial T}{\partial x} + v \frac{\partial T}{\partial y} \right) = \frac{\partial^2 T}{\partial y^2} \quad (2.1)$$

in the converging/diverging channel $-1 \leq x \leq 1$, $-g(x) \leq y \leq g(x)$, subject to the boundary conditions

$$T = 0 \quad x = -1, \quad (2.2)$$

$$T = 0 \quad y = \pm g(x), \quad (2.3)$$

$$\frac{\partial T}{\partial x} = 0 \quad x = 1, \quad (2.4)$$

and the initial conditions

$$T(0, y, 0) = 1, \quad (2.5)$$

$$T(x, y, 0) = 0, \quad x \neq 0. \quad (2.6)$$

Here T denotes nondimensional temperature, Pe is a (re-

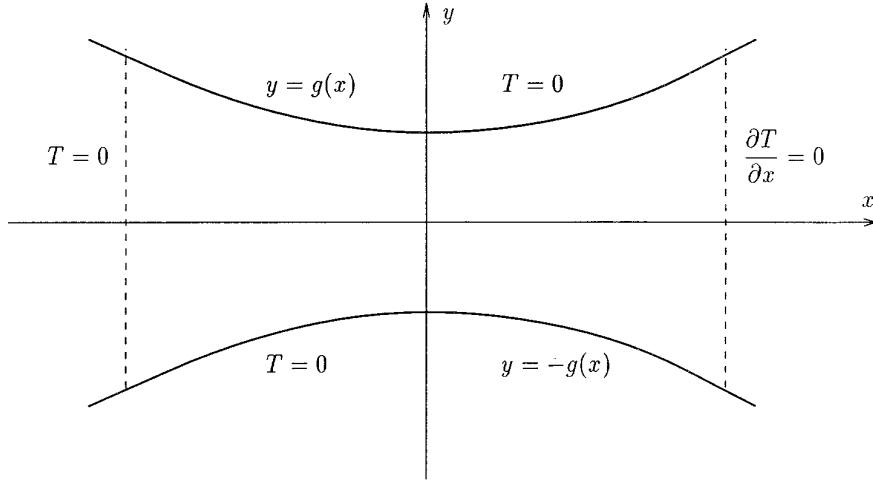


FIG. 1. Boundary conditions on the physical space \mathcal{P} .

duced) Peclet number, and u and v are known functions of x , y and represent the components of velocity in the x and y directions respectively. The solution domain is illustrated in Fig. 1.

2.2. Generalised Curvilinear Coordinates

The use of boundary fitted coordinates allows the problem to be solved in a considerably simpler rectangular geometry in a new space at the expense of increasing the complexity of the equation. Denoting the original physical space by \mathcal{P} , and the computational space by \mathcal{C} , we require the transformation of (2.1) under the mapping M : $(x, y, t) \rightarrow (\xi(x, y), \eta(x, y), t)$ from \mathcal{P} to \mathcal{C} . A simple application of the chain rule and division by $|\mathbf{J}|$, the determinant of the Jacobian matrix of the transformation, yields

$$\begin{aligned} & \frac{1}{|\mathbf{J}|} \frac{\partial T}{\partial t} + \left[\text{Pe} \left(u \frac{\xi_x}{|\mathbf{J}|} + v \frac{\xi_y}{|\mathbf{J}|} \right) - \frac{\xi_{yy}}{|\mathbf{J}|} \right] T_\xi \\ & + \left[\text{Pe} \left(u \frac{\eta_x}{|\mathbf{J}|} + v \frac{\eta_y}{|\mathbf{J}|} \right) - \frac{\eta_{yy}}{|\mathbf{J}|} \right] T_\eta \quad (2.7) \\ & = \frac{(\xi_y)^2}{|\mathbf{J}|} T_{\xi\xi} + \frac{2\eta_y \xi_y}{|\mathbf{J}|} T_{\xi\eta} + \frac{(\eta_y)^2}{|\mathbf{J}|} T_{\eta\eta}, \end{aligned}$$

or in conservative form

$$\begin{aligned} & \frac{1}{|\mathbf{J}|} \frac{\partial T}{\partial t} + \left[\text{Pe} \left(u \left(\frac{\xi_x T}{|\mathbf{J}|} \right)_\xi + v \left(\frac{\xi_y T}{|\mathbf{J}|} \right)_\xi \right) + \left(\frac{\xi_{yy} T}{|\mathbf{J}|} \right)_\xi \right] \\ & + \left[\text{Pe} \left(u \left(\frac{\eta_x T}{|\mathbf{J}|} \right)_\eta + v \left(\frac{\eta_y T}{|\mathbf{J}|} \right)_\eta \right) + \left(\frac{\eta_{yy} T}{|\mathbf{J}|} \right)_\eta \right] \quad (2.8) \\ & = \left(\frac{\xi_y^2 T}{|\mathbf{J}|} \right)_{\xi\xi} + \left(\frac{2\xi_y \eta_y T}{|\mathbf{J}|} \right)_{\xi\eta} + \left(\frac{\eta_y^2 T}{|\mathbf{J}|} \right)_{\eta\eta}. \end{aligned}$$

This is the form of the equation solved numerically on a regular rectangular grid in \mathcal{C} , where in practice ξ_x , ξ_y , ξ_{yy} , η_x , η_y , η_{yy} , are evaluated in terms of x_ξ , x_η , y_ξ , y_η , $x_{\xi\xi}$, $x_{\xi\eta}$, $x_{\eta\eta}$, $y_{\xi\xi}$, $y_{\xi\eta}$, $y_{\eta\eta}$. It will be demonstrated in Section 4.1 that for the particular mapping technique used here \mathbf{J} is non-singular. We note that Eq. (2.1) remains parabolic when transformed to general curvilinear coordinates provided that M is sufficiently differentiable. Indeed the discriminant $b^2 - 4ac$ of the second order partial differential equation

$$\frac{\partial T}{\partial t} = a \frac{\partial^2 T}{\partial x^2} + b \frac{\partial^2 T}{\partial x \partial y} + c \frac{\partial^2 T}{\partial y^2} \quad (2.9)$$

is transformed to

$$\begin{aligned} & \left[2a \frac{\partial \xi}{\partial x} \frac{\partial \eta}{\partial x} + 2c \frac{\partial \xi}{\partial y} \frac{\partial \eta}{\partial y} + b \left(\frac{\partial \xi}{\partial y} \frac{\partial \eta}{\partial x} + \frac{\partial \xi}{\partial x} \frac{\partial \eta}{\partial y} \right) \right]^2 \\ & - 4 \left(a \left(\frac{\partial \xi}{\partial x} \right)^2 + c \left(\frac{\partial \xi}{\partial y} \right)^2 + b \frac{\partial \xi}{\partial x} \frac{\partial \xi}{\partial y} \right) \\ & \times \left(a \left(\frac{\partial \eta}{\partial x} \right)^2 + c \left(\frac{\partial \eta}{\partial y} \right)^2 + b \frac{\partial \eta}{\partial x} \frac{\partial \eta}{\partial y} \right) \\ & = (b^2 - 4ac) \left[\frac{\partial \xi}{\partial x} \frac{\partial \eta}{\partial y} - \frac{\partial \xi}{\partial y} \frac{\partial \eta}{\partial x} \right]^2 = (b^2 - 4ac) |\mathbf{J}|^2, \end{aligned}$$

under the mapping M , so the sign of the discriminant is preserved providing $|\mathbf{J}|$ is non-zero.

3. THE NUMERICAL SCHEME

Several authors have considered the solution of parabolic equations with mixed derivatives of the form given

by Eq. (2.9) without lower order derivatives. Lax and Richtmyer [9] proposed a one-parameter scheme which requires the solution of an implicit system of equations in general for which relaxation methods were suggested. Douglas and Gunn [5] proposed an ADI method which requires the solution of four tridiagonal sets of equations at each time step. Several Russian authors have suggested a variety of “fractional step” schemes (sometimes called locally one-dimensional schemes) and have shown that the numerical solution can be reduced to the solution of two tridiagonal matrix equations per time step in the case of two spatial dimensions; see for instance Samarskii [12] and Andreev [1]. McKee and Mitchell [10] have derived an equally effective unconditionally stable ADI scheme for this two-dimensional case. Heron [8] has established convergence results for N -dimensional fractional step methods. In an alternative approach, Warming and Beam [15] used A-stable linear multistep methods to time-difference together with the method of approximate factorisation to construct unconditionally stable ADI schemes for mixed hyperbolic–parabolic partial differential equations which are first order accurate in time. Beam and Warming [2] used a similar approach to construct unconditionally stable schemes for parabolic partial differential equations which are second order accurate in time. More recently Craig and Sneyd [3] have demonstrated an unconditionally stable scheme for N -dimensional parabolic equations with mixed derivatives and in [4] have also derived an ADI scheme for a system of parabolic equations with mixed derivatives which is shown to be unconditionally stable if asymmetries in the coupling matrix are not too large.

For the parabolic equation (1.1) we propose the alternating direction implicit scheme given in Douglas-Rachford split form by the difference equations

$$\begin{aligned} & \left[1 - \frac{ra}{2} \delta_x^2 + \frac{pu}{2} \nabla_x \right] T_{i,j}^{n+1*} \\ &= \left[1 + rc\delta_y^2 - pv\nabla_y + \frac{ra}{2} \delta_x^2 - \frac{pu}{2} \nabla_x \right. \\ & \quad \left. + \frac{rb}{4} \delta_{xy} \right] T_{i,j}^n, \end{aligned} \quad (3.1a)$$

$$\begin{aligned} & \left[1 - \frac{rc}{2} \delta_y^2 + \frac{pv}{2} \nabla_y \right] T_{i,j}^{n+1} \\ &= T_{i,j}^{n+1*} - \left[\frac{rc}{2} \delta_y^2 - \frac{pv}{2} \nabla_y \right] T_{i,j}^n, \end{aligned} \quad (3.1b)$$

in which $T_{i,j}^n$ is our approximation to $T(i \Delta x, j \Delta y, n \Delta t)$, where $\Delta x = \Delta y$ defines a uniform spatial mesh with ratios

$$r = \Delta t/(\Delta x)^2 = \Delta t/(\Delta y)^2, \quad p = \Delta t/\Delta x,$$

and we define the operations

$$\begin{aligned} \delta_x^2 T_{i,j}^n &= T_{i+1,j}^n - 2T_{i,j}^n + T_{i-1,j}^n, \\ \delta_{xy} T_{i,j}^n &= T_{i+1,j+1}^n - T_{i+1,j-1}^n - T_{i-1,j+1}^n + T_{i-1,j-1}^n, \\ \nabla_x T_{i,j}^n &= T_{i,j}^n - T_{i-1,j}^n, \end{aligned}$$

with corresponding definitions for δ_y^2 and ∇_y . The scheme treats the second order derivatives in the same way as McKee and Mitchell [10]; indeed, the two schemes are identical in the special case when $u = v = 0$. The scheme may be written in the unsplit form

$$\begin{aligned} & \left[1 - \frac{ra}{2} \delta_x^2 + \frac{pu}{2} \nabla_x \right] \left[1 - \frac{rc}{2} \delta_y^2 + \frac{pv}{2} \nabla_y \right] T_{i,j}^{n+1} \\ &= \left\{ \left[1 + \frac{ra}{2} \delta_x^2 - \frac{pu}{2} \nabla_x \right] \left[1 + \frac{rc}{2} \delta_y^2 - \frac{pv}{2} \nabla_y \right] \right. \\ & \quad \left. + \frac{rb}{4} \delta_{xy} \right\} T_{i,j}^n. \end{aligned} \quad (3.2)$$

The scheme is equivalent to one developed using the method of approximate factorisation using the one-step trapezoidal formula to time-difference in the style of Warming and Beam [15].

In the special case where u and v are identically zero the scheme is consistent to order $O(\Delta t + (\Delta x)^2)$ but more generally is of order $O(\Delta t + \Delta x)$; however, this order of accuracy can be improved to $O(\Delta t + (\Delta x)^2)$ by introducing the second order upwinding operation

$$\nabla_x T_{i,j}^n = \frac{3}{2} T_{i,j}^n - 2T_{i-1,j}^n + \frac{1}{2} T_{i-2,j}^n, \quad (3.3)$$

with a corresponding definition for the operator ∇_y . Higher order upwinding is of little value as the second order spatial derivative approximations are only second order accurate.

3.1. Stability Analysis for Constant Coefficients

We use the traditional von Neumann method to analyse the stability of the scheme given by Eq. (3.2), which is applicable in the special case when the coefficients a, b, c, u and v are constant. We consider a solution to the difference equation (3.2) given by

$$T_{i,j}^n = A e^{\alpha n \Delta t} e^{\sqrt{-1}\beta i \Delta x} e^{\sqrt{-1}\gamma j \Delta y},$$

where β and γ are constant wavenumbers. If periodic boundary conditions are assumed the von Neumann condition for stability requires $|e^{\alpha \Delta t}| \leq 1$ for all β, γ . It is straightforward to show that

$$\begin{aligned}\delta_x^2 T_{i,j}^n &= 2[\cos(\beta \Delta x) - 1] T_{i,j}^n, \\ \delta_y^2 T_{i,j}^n &= 2[\cos(\gamma \Delta y) - 1] T_{i,j}^n, \\ \nabla_x T_{i,j}^n &= [1 - \cos(\beta \Delta x) + \sqrt{-1} \sin(\beta \Delta x)] T_{i,j}^n, \\ \nabla_y T_{i,j}^n &= [1 - \cos(\gamma \Delta y) + \sqrt{-1} \sin(\gamma \Delta y)] T_{i,j}^n, \\ \delta_{xy} T_{i,j}^n &= -4 \sin(\gamma \Delta y) \sin(\beta \Delta x) T_{i,j}^n,\end{aligned}$$

which, upon substitution into the scheme given by Eq. (3.2), yield the amplification factor

$$|e^{\alpha \Delta t}| = \left| \frac{z_1 z_2 + z_0}{z_3 z_4} \right|,$$

where

$$\begin{aligned}z_0 &= -4br \sin(\beta \Delta x) \sin(\gamma \Delta y) \\ z_1 &= [2 - (2ar + pu)(1 - \cos(\beta \Delta x)) \\ &\quad - \sqrt{-1} pu \sin(\beta \Delta x)], \\ z_2 &= [2 - (2cr + pv)(1 - \cos(\gamma \Delta y)) \\ &\quad - \sqrt{-1} pv \sin(\gamma \Delta y)], \\ z_3 &= [2 + (2ar + pu)(1 - \cos(\gamma \Delta y)) \\ &\quad + \sqrt{-1} pv \sin(\gamma \Delta y)], \\ z_4 &= [2 + (2ar + pu)(1 - \cos(\beta \Delta x)) \\ &\quad + \sqrt{-1} pu \sin(\beta \Delta x)].\end{aligned}$$

Clearly the von Neumann condition for stability may be equivalently written as $F := |z_3 z_4|^2 - |z_1 z_2 + z_0|^2 \geq 0$ for all β and γ . Evaluating F gives

$$\begin{aligned}F(a, b, c, u, v, r, p, \theta, \phi) &= p^2 u^2 (2cr + pv) \sin^2 \theta \sin^2 \left(\frac{\phi}{2}\right) \\ &\quad + p^2 v^2 (2ar + pu) \sin^2 \left(\frac{\theta}{2}\right) \sin^2 \phi \\ &\quad + 4 \left[(2ar + pu) \sin^2 \left(\frac{\theta}{2}\right) + (2cr + pv) \sin^2 \left(\frac{\phi}{2}\right) \right] \\ &\quad \times \left[1 + (2ar + pu)(2cr + pv) \sin^2 \left(\frac{\theta}{2}\right) \sin^2 \left(\frac{\phi}{2}\right) \right] \\ &\quad + br \sin \theta \sin \phi \left\{ 2 \left[1 - (2ar + pu) \sin^2 \left(\frac{\theta}{2}\right) \right] \right. \\ &\quad \times \left[1 - (2cr + pv) \sin^2 \left(\frac{\phi}{2}\right) \right] \\ &\quad \left. - \frac{p^2 uv}{2} \sin \theta \sin \phi - br \sin \theta \sin \phi \right\},\end{aligned}\tag{3.4}$$

where we have introduced

$$\theta = \beta \Delta x, \quad \phi = \gamma \Delta y.$$

Writing

$$\begin{aligned}F(a, b, c, u, v, r, p, \theta, \phi) &= [F(a, b, c, u, v, r, p, \theta, \phi) \\ &\quad - F(a, b, c, 0, 0, r, p, \theta, \phi)] + F(a, b, c, 0, 0, r, p, \theta, \phi),\end{aligned}\tag{3.5}$$

it is clear that in order to demonstrate unconditional stability of the scheme given by Eq. (3.2), it is sufficient to show that both terms of the sum in the expression (3.5) are non-negative. However, in the case $u = v = 0$, the scheme reduces to the McKee–Mitchell scheme given in [10] and this scheme is demonstrated to be unconditionally stable, or equivalently

$$F(a, b, c, 0, 0, r, p, \theta, \phi) \geq 0.$$

Thus we need only show that

$$\begin{aligned}D(a, b, c, u, v, r, p, \theta, \phi) &:= F(a, b, c, u, v, r, p, \theta, \phi) \\ &\quad - F(a, b, c, 0, 0, r, p, \theta, \phi) \geq 0.\end{aligned}$$

We will require the following three inequalities.

LEMMA 1.

$$a \sin^2 \left(\frac{\theta}{2}\right) + c \sin^2 \left(\frac{\phi}{2}\right) + \frac{b}{4} \sin \theta \sin \phi \geq 0.$$

This is clearly true if $b \sin \theta \sin \phi \geq 0$; otherwise, since $b^2 < 4ac$,

$$\begin{aligned}a \sin^2 \left(\frac{\theta}{2}\right) + c \sin^2 \left(\frac{\phi}{2}\right) + \frac{b}{4} \sin \theta \sin \phi &> a \sin^2 \left(\frac{\theta}{2}\right) \\ &\quad + c \sin^2 \left(\frac{\phi}{2}\right) - \frac{\sqrt{ac}}{2} |\sin \theta \sin \phi| \\ &\geq \left(\sqrt{c} \left| \sin \left(\frac{\phi}{2}\right) \right| - \sqrt{a} \left| \sin \left(\frac{\theta}{2}\right) \right| \right)^2 \geq 0.\end{aligned}$$

LEMMA 2.

$$1 + 4r^2ac \sin^2\left(\frac{\theta}{2}\right) \sin^2\left(\frac{\phi}{2}\right) - \frac{br}{2} \sin \theta \sin \phi \geq 0.$$

Clearly this is true if $b \sin \theta \sin \phi \leq 0$; otherwise

$$\begin{aligned} 1 + 4r^2ac \sin^2\left(\frac{\theta}{2}\right) \sin^2\left(\frac{\phi}{2}\right) - \frac{br}{2} \sin \theta \sin \phi \\ > 1 + 4r^2ac \sin^2\left(\frac{\theta}{2}\right) \sin^2\left(\frac{\phi}{2}\right) - r\sqrt{ac} |\sin \theta \sin \phi|, \end{aligned} \quad (3.6)$$

but

$$\begin{aligned} 1 + 4r^2ac \sin^2\left(\frac{\theta}{2}\right) \sin^2\left(\frac{\phi}{2}\right) - r\sqrt{ac} |\sin \theta \sin \phi| \\ = \left(2r\sqrt{ac} \left| \sin\left(\frac{\theta}{2}\right) \sin\left(\frac{\phi}{2}\right) \right| - \left| \cos\left(\frac{\theta}{2}\right) \cos\left(\frac{\phi}{2}\right) \right|\right)^2 \\ + 1 - \left(\cos\left(\frac{\theta}{2}\right) \cos\left(\frac{\phi}{2}\right)\right)^2 \geq 0. \end{aligned}$$

LEMMA 3.

$$u^2c + v^2a - uwb \cos^2\left(\frac{\theta}{2}\right) \cos^2\left(\frac{\phi}{2}\right) \geq 0.$$

Clearly this is true if $b \leq 0$; otherwise

$$\begin{aligned} u^2c + v^2a - uwb \cos^2\left(\frac{\theta}{2}\right) \cos^2\left(\frac{\phi}{2}\right) \\ \geq u^2c + v^2a - 2uw\sqrt{ac} \cos^2\left(\frac{\theta}{2}\right) \cos^2\left(\frac{\phi}{2}\right). \end{aligned}$$

But

$$u^2c + v^2a - 2uw\sqrt{ac} \cos^2\left(\frac{\theta}{2}\right) \cos^2\left(\frac{\phi}{2}\right) \geq (u\sqrt{c} - v\sqrt{a})^2 \geq 0.$$

It is straightforward to show that $D(a, b, c, u, v, r, p, \theta, \phi)$ takes the form

$$D(a, b, c, u, v, r, p, \theta, \phi)$$

$$\begin{aligned} &= p^2u^2(2cr + pv) \sin^2 \theta \sin^2\left(\frac{\phi}{2}\right) \\ &\quad + p^2v^2(2ar + pu) \sin^2\left(\frac{\theta}{2}\right) \sin^2 \phi \\ &\quad + 4 \left[(2arpv + 2crpu + p^2uw) \sin^2\left(\frac{\theta}{2}\right) \sin^2\left(\frac{\phi}{2}\right) \right] \\ &\quad \times \left[2ar \sin^2\left(\frac{\theta}{2}\right) + 2cr \sin^2\left(\frac{\phi}{2}\right) \right] \\ &\quad + 4 \left[1 + (2ar + pu)(2cr + pv) \sin^2\left(\frac{\theta}{2}\right) \sin^2\left(\frac{\phi}{2}\right) \right] \\ &\quad \times \left[pv \sin^2\left(\frac{\phi}{2}\right) + pu \sin^2\left(\frac{\theta}{2}\right) \right] + br \sin \theta \sin \phi \\ &\quad \times \left\{ 2 \left[(2arpv + 2crpu + p^2uw) \sin^2\left(\frac{\theta}{2}\right) \sin^2\left(\frac{\phi}{2}\right) \right. \right. \\ &\quad \left. \left. - pu \sin^2\left(\frac{\theta}{2}\right) - pv \sin^2\left(\frac{\phi}{2}\right) \right] - \frac{p^2uw}{2} \sin \theta \sin \phi \right\}. \end{aligned} \quad (3.7)$$

Equation (3.7) may be rearranged as

$$D(a, b, c, u, v, r, p, \theta, \phi)$$

$$\begin{aligned} &= 8r \left[(2arpv + 2crpu + p^2uw) \sin^2\left(\frac{\theta}{2}\right) \sin^2\left(\frac{\phi}{2}\right) \right] \\ &\quad \times \left[c \sin^2\left(\frac{\phi}{2}\right) + a \sin^2\left(\frac{\theta}{2}\right) + \frac{b}{4} \sin \theta \sin \phi \right] \\ &\quad + 4 \left[pv \sin^2\left(\frac{\phi}{2}\right) + pu \sin^2\left(\frac{\theta}{2}\right) \right] \\ &\quad \times \left[1 + 4r^2ac \sin^2\left(\frac{\theta}{2}\right) \sin^2\left(\frac{\phi}{2}\right) - \frac{br}{2} \sin \theta \sin \phi \right] \\ &\quad + 8p^2r \sin^2\left(\frac{\phi}{2}\right) \sin^2\left(\frac{\theta}{2}\right) \\ &\quad \times \left[u^2c + v^2a - uwb \cos^2\left(\frac{\theta}{2}\right) \cos^2\left(\frac{\phi}{2}\right) \right] \\ &\quad + 4 \sin^2\left(\frac{\phi}{2}\right) \sin^2\left(\frac{\theta}{2}\right) \\ &\quad \times \left[p^3uw(u + v) + 2rp^2uw \left(c \sin^2\left(\frac{\phi}{2}\right) + a \sin^2\left(\frac{\theta}{2}\right) \right) \right], \end{aligned} \quad (3.8)$$

which, using the results of Lemmata 1, 2, and 3, is clearly

non-negative and hence the scheme given in Eq. (3.2) is unconditionally stable. The scheme is also unconditionally stable when the second order upwinding scheme given in Eq. (3.3) is applied to the convection terms; the proof is similar to that for the first order upwinding approximation and is detailed in the Appendix.

3.2. The Scheme in N Dimensions

For the N -dimensional heat-transport equation

$$\frac{\partial T}{\partial t} + \sum_{i=1}^N u_i \frac{\partial T}{\partial x_i} = \sum_{i=1}^N \sum_{j=1}^i a_{i,j} \frac{\partial^2 T}{\partial x_i \partial x_j},$$

where parabolicity implies that the matrix A whose i, j th entry is $(A)_{i,j} = (1 + \delta_{ij})a_{i,j}/2$ is positive definite, we extend the scheme given by Eq. (3.2) to

$$\begin{aligned} & \prod_{j=1}^N (1 - D_j) T_{i_1, \dots, i_N}^{n+1} \\ &= \left[2 \sum_{j=1}^N E_j + \frac{1}{4} r \sum_{i=2}^N \sum_{j=1}^{i-1} a_{i,j} \delta_{x_i x_j} \right. \\ & \quad \left. + \prod_{j=1}^N (1 - D_j) \right] T_{i_1, \dots, i_N}^n, \end{aligned} \quad (3.9)$$

where

$$E_j = \frac{r}{2} a_{jj} \delta_{x_j}^2 - \frac{pu_j}{2} \nabla_{x_j}$$

and we may choose $D_j = D_j^I$ or D_j^{II} , where

$$\begin{aligned} D_j^I &= \lambda \frac{r}{2} a_{jj} \delta_{x_j}^2 - \frac{pu_j}{2} \nabla_{x_j}, \\ D_j^{II} &= \lambda \left(\frac{r}{2} a_{jj} \delta_{x_j}^2 - \frac{pu_j}{2} \nabla_{x_j} \right). \end{aligned}$$

The scheme may be split as

$$\begin{aligned} [1 - D_1] T_{i_1, \dots, i_N}^{n+1(1)} &= \left[1 - D_1 + 2 \sum_{j=1}^N E_j \right. \\ & \quad \left. + \frac{1}{4} \sum_{i=2}^N \sum_{j=1}^{i-1} a_{i,j} \delta_{x_i x_j} \right] T_{i_1, \dots, i_N}^n, \\ [1 - D_2] T_{i_1, \dots, i_N}^{n+1(2)} &= T_{i_1, \dots, i_N}^{n+1(1)} - D_2 T_{i_1, \dots, i_N}^n, \\ & \vdots \\ [1 - D_N] T_{i_1, \dots, i_N}^{n+1} &= T_{i_1, \dots, i_N}^{n+1(N-1)} - D_N T_{i_1, \dots, i_N}^n. \end{aligned} \quad (3.10)$$

Applying von Neumann stability analysis as before we substitute

$$T_{i_1, \dots, i_N}^n = A e^{an \Delta t} \prod_{j=1}^N e^{\sqrt{-1} \beta_j i_j \Delta x_j}$$

into Eq. (3.9) and find unconditional stability if and only if $F \geq 0$ for all $\theta_1, \theta_2, \dots, \theta_N$, where

$$\begin{aligned} F := & \left(\left| \prod_{j=1}^N (1 - D_j) T_{i_1, \dots, i_N}^n \right|^2 \right. \\ & - \left[2 \sum_{j=1}^N E_j + \frac{1}{4} \sum_{i=2}^N \sum_{j=1}^{i-1} a_{i,j} \delta_{x_i x_j} \right. \\ & \left. \left. + \prod_{j=1}^N (1 - D_j) \right] T_{i_1, \dots, i_N}^n \right|^2 \Big) / |T_{i_1, \dots, i_N}^n|^2 \end{aligned}$$

When $N = 2$, the choice $\lambda = 1$ recovers the scheme given by Eq. (3.2). The introduction of the real parameter λ is necessary if unconditional stability is sought since in the special case of no convection terms the scheme given by Eq. (3.9) defaults to that of Craig and Sneyd [3] who found the necessary and sufficient condition

$$\lambda \geq \lambda_c(N) \quad (3.11)$$

for unconditional stability, where for example $\lambda_c(2) = 1$ and $\lambda_c(3) = 4/3$. Clearly condition (3.11) is a necessary condition for the present scheme to be unconditionally stable; it is not, however, sufficient in general since when $N = 2$, for example, values of $\lambda > \lambda_c(2)$ have been found such that F is negative for some values of θ_1, θ_2 . In short, it is still not clear whether an unconditionally stable scheme exists for solving the general N -dimensional heat transport equation.

4. AN APPLICATION OF THE SCHEME TO THE DYE LASER PROBLEM

4.1. The Mapping From \mathcal{C} to \mathcal{P}

An algebraic method is used to map the regular finite difference grid in \mathcal{C} onto the boundary-fitted grid in \mathcal{P} which is more fully described in Fletcher [7], for example. We schematically illustrate the mapping in Fig. 2. The method relies on four one-dimensional stretching functions, r_{AB} , r_{DC} , s_{AD} , and s_{BC} , which map the regularly distributed nodes on boundaries $A'B'$, $D'C'$, $A'D'$, and $B'C'$ in \mathcal{C} onto (in general) irregularly distributed nodes on the corresponding boundaries AB , DC , AD , and BC in \mathcal{P} . The stretching functions are smooth mappings of the interval $[0, 1]$ onto itself and are chosen to cluster grid

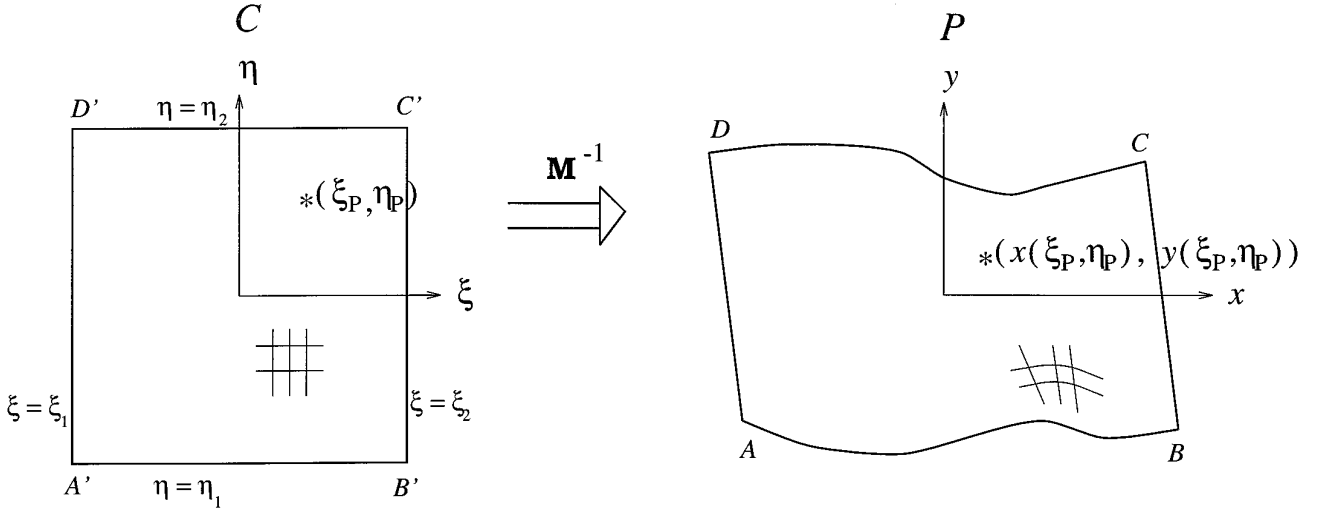


FIG. 2. The mapping from \mathcal{C} to \mathcal{P} .

cells in areas of greatest computational interest near the boundary walls in the η direction and in the narrowest section of the channel in the ξ direction. The interior nodes in \mathcal{P} are then obtained from an interpolation from these boundary nodes. Defining the functions representing the boundary walls DC and AB parametrically by

$$\begin{aligned} \{(x_{DC}(\alpha), y_{DC}(\alpha)) : \alpha \in [0, 1]\}, \\ \{(x_{AB}(\beta), y_{AB}(\beta)) : \beta \in [0, 1]\} \end{aligned} \quad (4.1)$$

(where $(x_{DC}(0), y_{DC}(0)) = (x_D, y_D)$, $(x_{DC}(1), y_{DC}(1)) = (x_C, y_C)$ and similarly $(x_{AB}(0), y_{AB}(0)) = (x_A, y_A)$, $(x_{AB}(1), y_{AB}(1)) = (x_B, y_B)$) the mapping from \mathcal{C} to \mathcal{P} is given by

$$x(\xi, \eta) = (1 - S(\xi^*, \eta^*))x_{AB}(r_{AB}(\xi^*)) + S(\xi^*, \eta^*)x_{DC}(r_{DC}(\xi^*)), \quad (4.2)$$

$$y(\xi, \eta) = (1 - S(\xi^*, \eta^*))y_{AB}(r_{AB}(\xi^*)) + S(\xi^*, \eta^*)y_{DC}(r_{DC}(\xi^*)), \quad (4.3)$$

where

$$S(\xi^*, \eta^*) = s_{AD}(\eta^*) + \xi^*(s_{BC}(\eta^*) - s_{AD}(\eta^*))$$

and

$$\xi^* = \frac{\xi - \xi_1}{\xi_2 - \xi_1}, \quad \eta^* = \frac{\eta - \eta_1}{\eta_2 - \eta_1}.$$

However, for the problem under consideration, we have symmetry about the x axis in \mathcal{P} and so

$$\begin{aligned} x_w(\alpha) &:= x_{AB}(\alpha) = x_{DC}(\alpha), \\ y_w(\alpha) &:= -y_{AB}(\alpha) = y_{DC}(\alpha) > 0, \end{aligned}$$

for $\alpha \in [0, 1]$. Furthermore our example converging/diverging channel appropriate for a dye laser cell is symmetrical about the y axis in \mathcal{P} so that appropriate stretching functions satisfy

$$\begin{aligned} s_{AD}(\eta^*) = s_{BC}(\eta^*) &:= s(\eta^*) = 1 - s(1 - \eta^*), \\ r_{AB}(\xi^*) = r_{DC}(\xi^*) &:= r(\xi^*) = 1 - r(1 - \xi^*). \end{aligned}$$

Further details of the stretching functions used in these calculations are given in Section 4.3. The mappings (4.2) and (4.3) therefore reduce to

$$x(\xi, \eta) = x_w(r(\xi^*)), \quad (4.4)$$

$$y(\xi, \eta) = [2s(\eta^*) - 1]y_w(r(\xi^*)). \quad (4.5)$$

We note that $|\mathbf{J}^{-1}|$ has no zeroes or singularities on the domain of interest (and hence neither does $|\mathbf{J}|$) since

$$|\mathbf{J}^{-1}| = x_\xi y_\eta - x_\eta y_\xi = 2 \frac{dx_w}{dr} \frac{dr}{d\xi^*} \frac{d\xi^*}{d\xi} \frac{ds}{d\eta^*} \frac{d\eta^*}{d\eta} y_w(r(\xi^*))$$

and all of the factors in the above expression are positive and have no singularities.

4.2. Discretisation

Equation (2.8) may be re-written as

$$\begin{aligned} \frac{\partial T}{\partial t} + |\mathbf{J}| \text{Pe} [u \{ (Ty_\eta)_\xi - (Ty_\xi)_\eta \} \\ + v \{ (Tx_\xi)_\eta - (Tx_\eta)_\xi \}] + |\mathbf{J}| (fT)_\xi \\ + |\mathbf{J}| (gT)_\eta = |\mathbf{J}| [(aT)_{\xi\xi} + (bT)_{\xi\eta} + (cT)_{\eta\eta}], \end{aligned} \quad (4.6)$$

where

$$|\mathbf{J}^{-1}| a(\xi, \eta) = x_\eta^2, \quad (4.7)$$

$$|\mathbf{J}^{-1}| b(\xi, \eta) = -2x_\eta x_\xi, \quad (4.8)$$

$$|\mathbf{J}^{-1}| c(\xi, \eta) = x_\xi^2, \quad (4.9)$$

$$\begin{aligned} |\mathbf{J}^{-1}|^2 f(\xi, \eta) = x_\eta^2 (x_\eta y_{\xi\xi} - y_\eta x_{\xi\xi}) - 2x_\xi x_\eta (x_\eta y_{\xi\eta} - y_\eta x_{\xi\eta}) \\ + x_\xi^2 (y_\eta x_{\eta\eta} - x_\eta y_{\eta\eta}), \end{aligned} \quad (4.10)$$

$$\begin{aligned} |\mathbf{J}^{-1}|^2 g(\xi, \eta) = x_\eta^2 (y_\xi x_{\xi\xi} - x_\xi y_{\xi\xi}) - 2x_\xi x_\eta (y_\xi x_{\xi\eta} - x_\xi y_{\xi\eta}) \\ + x_\xi^2 (y_\xi x_{\eta\eta} - x_\xi y_{\eta\eta}), \end{aligned} \quad (4.11)$$

Equation (4.6) was solved using the ADI method given in split form by (3.1). Thus, the following difference equations were solved,

$$\begin{aligned} \left[1 - \frac{r|\mathbf{J}|}{2} \delta_x^2 a_{i,j} + \frac{p|\mathbf{J}|}{2} \nabla_x f_{i,j} + \frac{\text{Pep}|\mathbf{J}|}{2} u_{i,j} \nabla_x y_{\eta_{i,j}} \right. \\ \left. - \frac{\text{Pep}|\mathbf{J}|}{2} v_{i,j} \nabla_x x_{\eta_{i,j}} \right] T_{i,j}^{n+1*} = [1 + r|\mathbf{J}| \delta_y^2 c_{i,j} - p|\mathbf{J}| \nabla_y g_{i,j} \\ - \text{Pep}|\mathbf{J}| v_{i,j} \nabla_y x_{\eta_{i,j}} + \text{Pep}|\mathbf{J}| u_{i,j} \nabla_y y_{\eta_{i,j}}] \\ + \frac{r|\mathbf{J}|}{2} \delta_x^2 a_{i,j} - \frac{p|\mathbf{J}|}{2} \nabla_x f_{i,j} - \frac{\text{Pep}|\mathbf{J}|}{2} u_{i,j} \nabla_x y_{\eta_{i,j}} \\ + \frac{\text{Pep}|\mathbf{J}|}{2} v_{i,j} \nabla_x x_{\eta_{i,j}} \\ + \frac{r|\mathbf{J}|}{4} \delta_{xy} b_{i,j} \left. \right] T_{i,j}^n, \end{aligned} \quad (4.12)$$

$$\begin{aligned} \left[1 - \frac{r|\mathbf{J}|}{2} \delta_y^2 c_{i,j} + \frac{p|\mathbf{J}|}{2} \nabla_y g_{i,j} - \frac{\text{Pep}|\mathbf{J}|}{2} u_{i,j} \nabla_y y_{\xi_{i,j}} \right. \\ \left. + \frac{\text{Pep}|\mathbf{J}|}{2} v_{i,j} \nabla_y x_{\xi_{i,j}} \right] T_{i,j}^{n+1} = T_{i,j}^{n+1*} - \left[\frac{r|\mathbf{J}|}{2} \delta_y^2 c_{i,j} \right. \\ \left. - \frac{p|\mathbf{J}|}{2} \nabla_y g_{i,j} + \frac{\text{Pep}|\mathbf{J}|}{2} u_{i,j} \nabla_y y_{\xi_{i,j}} - \frac{\text{Pep}|\mathbf{J}|}{2} v_{i,j} \nabla_y x_{\xi_{i,j}} \right] T_{i,j}^n, \end{aligned} \quad (4.13)$$

where

$$r = \Delta t / (\Delta \xi)^2 = \Delta t / (\Delta \eta)^2, \quad p = \Delta t / \Delta \xi.$$

4.3. Computational Details and Accuracy

For the results in this section we used the parabola

$$g(x) = 0.53 + 0.47x^2$$

to describe the shape of the walls, which is typical of the shape for the channel of a dye laser cell. The stretching functions used in the grid generation were the asymmetric double sided functions derived by Vinokur [14]. Specifically, if

$$s_0 = \frac{ds}{d\lambda} \Big|_{\lambda=0} = \frac{ds}{d\lambda} \Big|_{\lambda=1}$$

is given, then

$$s(\lambda) = \frac{\tanh[c_1(\lambda - 1/2)]}{2 \tanh(c_1/2)} + \frac{1}{2},$$

where c_1 is derived from solving

$$s_0 = \frac{\sinh c_1}{c_1},$$

and

$$r(\lambda) = \frac{\tan[c_2(\lambda - 1/2)]}{2 \tan(c_2/2)} + \frac{1}{2},$$

where c_2 is derived from solving

$$r_0 = \frac{\sin c_2}{c_2},$$

where

$$r_0 = \frac{dr}{d\lambda} \Big|_{\lambda=0} = \frac{dr}{d\lambda} \Big|_{\lambda=1}.$$

The values of r_0 and s_0 used here were 0.9 and 2.0, respectively. The velocity components used here are the well-known lubrication solutions

$$u(x, y) = \frac{3Q}{4g(x)} [g(x)^2 - y^2], \quad (4.14)$$

$$v(x, y) = \frac{3Qg'(x)y}{4g(x)^4} [g(x)^2 - y^2], \quad (4.15)$$

where

$$Q = \int_{-g(x)}^{g(x)} u(x, y) dy$$

is the constant volume flux per unit width along the channel. FORTRAN codes were written to implement the mapping described in Section 4.1 to generate the boundary-

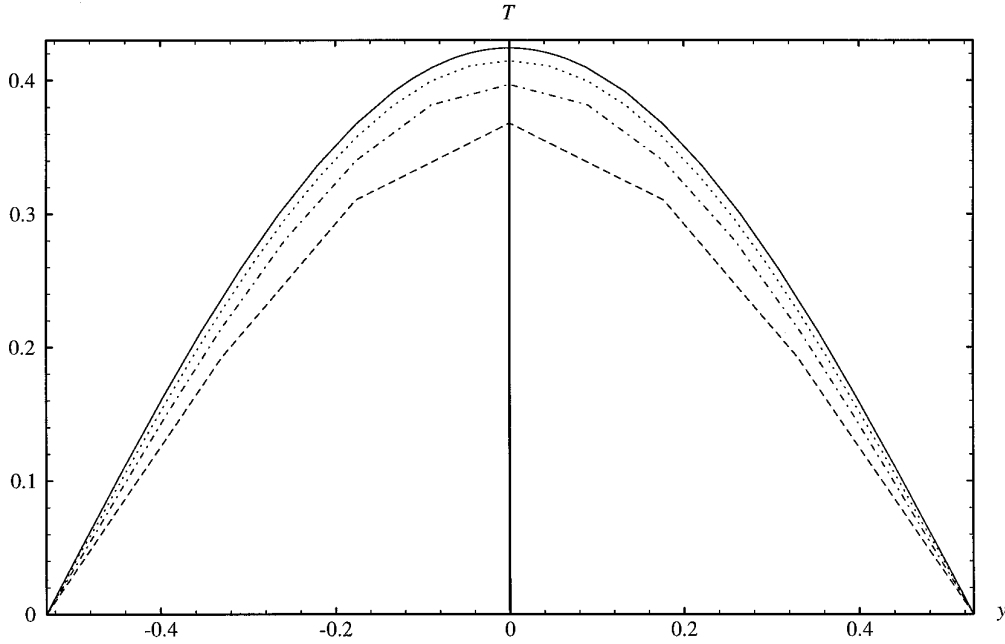


FIG. 3. Plots of $T(x=0, y, t=0.125)$; (—) exact solution, (\cdots) 32 grid cells, ($-\cdot-$) 16 grid cells, and ($---$) 8 grid cells. All numerical calculations were made with 25 time steps of size $\Delta t = 0.005$.

fitted grid and to apply the scheme given by Eqs. (4.12) and (4.13). Calculations were made on a DEC 3400S mainframe computer which typically took 8 s CPU time to generate a grid with 40 grid cells in either direction and calculate ten time steps.

The theoretical spatial accuracy of the scheme using the two-point upwind scheme for the convection terms is $O(\Delta x)$; we may obtain some indication of the accuracy of the scheme in practice by calculating the observed order of convergence of the solutions T_C , T_M , and T_F obtained from coarse, medium, and fine grids respectively, where the medium grid is obtained from the coarse grid by doubling the number of grid cells in either direction and this process is repeated to obtain the fine grid from the medium one. We thus have

$$T - T_F \approx k \Delta x^q, T - T_M \approx k(2 \Delta x)^q, T - T_C \approx k(4 \Delta x)^q.$$

Eliminating T , k we obtain the observed order

$$q \approx \log \left(\frac{T_F - T_M}{T_M - T_C} \right) / \log 2.$$

We calculate this observed order at points in the solution domain where the solution is non-zero and present some averaged values in Table I. The observed order appears to be close to the theoretical value.

In practice the scheme does exhibit a lack of stability for large enough grid Courant numbers; for instance, in solving on a grid with 40 cells in either direction when $Pe = 100$ requires Δt to be less than (approximately) 0.002. For comparison however, results were obtained with an explicit scheme which forward time-differenced and used centred differences and first order upwinding to approximate the second and first order spatial derivatives respectively. It was found that the explicit scheme required Δt to be typically a factor of 10 smaller than the corresponding ADI bound in order to maintain stability. It should be remembered, however, that von Neumann analysis guarantees stability in the case of constant coefficients of the equation and periodic boundary conditions; the present problem, however, has non-constant equation coefficients, non-periodic boundary conditions, and discontinuous ini-

TABLE I

Observed Order of Convergence of Scheme
for Various Values of Pe

Pe	q
0.1	1.222
1.0	1.068
10.0	0.924

Note. The coarse, medium, and fine grids consist of 10×10 , 20×20 , and 40×40 grid cells respectively and 5 time steps of size $\Delta t = 0.001$ were made. The theoretical value for q is 1.

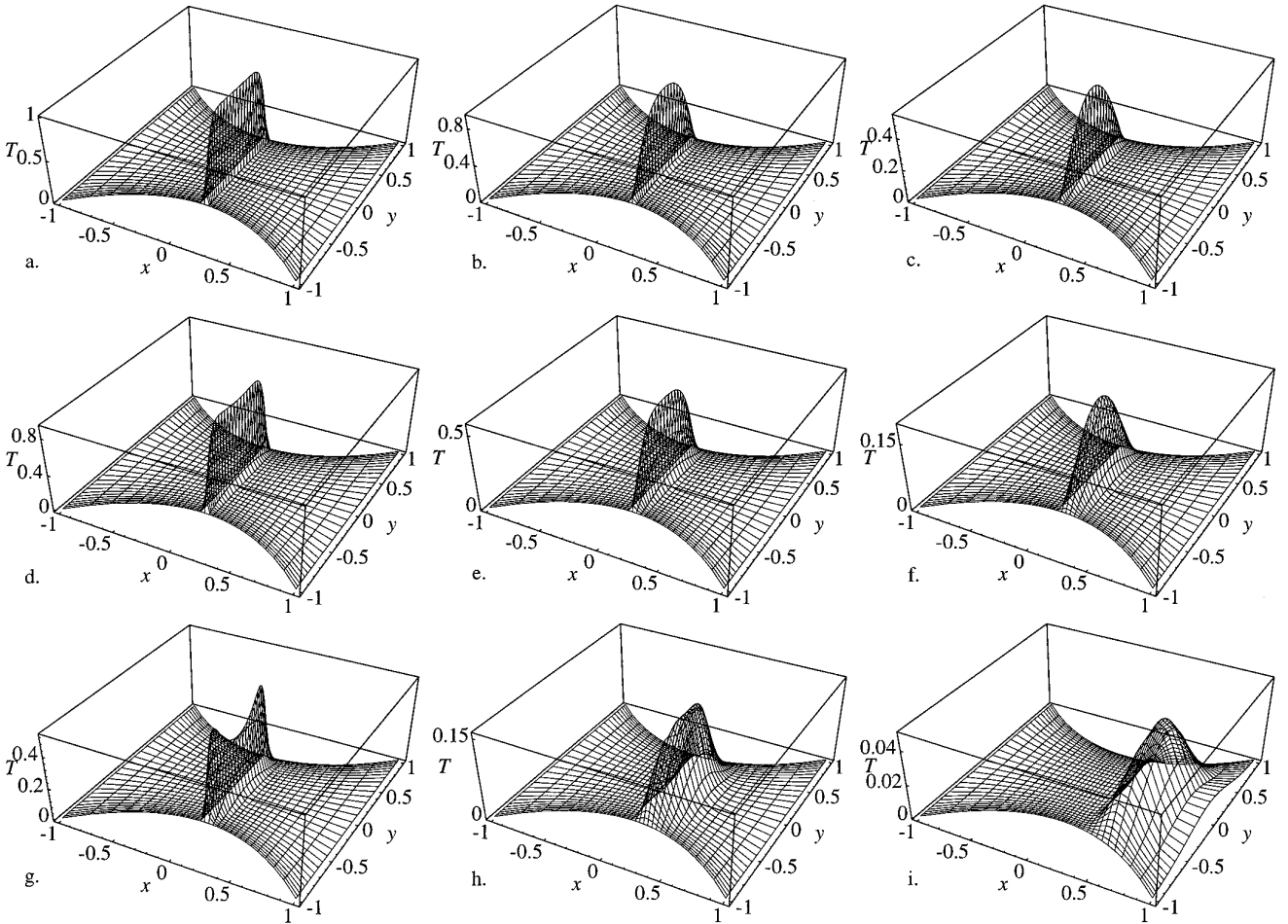


FIG. 4. Temperature of fluid in a model dye laser cell when (a, b, c) $Pe = 0.1$, (d, e, f) $Pe = 1$, and (g, h, i) $Pe = 10$ at times (a, d, g) $t = 0.004$, (b, e, h) $t = 0.022$, and (c, f, i) $t = 0.075$. All calculations were made on a grid of 30×30 grid cells with $\Delta t = 0.001$.

tial conditions. For both the explicit and the ADI scheme instability was manifested by rapidly growing disturbances near the discontinuities ($x = 0, y = \pm 1$) in the initial conditions.

4.4. Results

In the special case when $Pe = 0$ the exact solution

$$T(y, t) = \sum_{n=0}^{\infty} \frac{4(-1)^n}{(2n+1)\pi} \cos(\alpha_n y e)^{-\alpha_n^2 t},$$

where

$$\alpha_n = \frac{(2n+1)\pi}{2g(0)},$$

is easily derived. In this case, since there is no convection (or diffusion) in the x direction, we are solving the one-

dimensional diffusion equation on $x = 0$. Numerical solutions for various numbers of grid nodes together with the exact solution are plotted in Fig. 3, which demonstrates convergence of the solution under grid refinement in this case. For $Pe = 0.1, 1$, and 10 we plot in Fig. 4 numerical solutions of Eq. (4.6) obtained through application of the scheme (4.12), (4.13) at three ‘‘snapshot’’ times. For $Pe = 1.0$, the initial pulse evolves in time as shown in Figs. 4d–4f. Typically the effect of convection is initially to cause the formation of a trough in the temperature profile, because heated fluid is swept away faster from the centre of the channel, leaving temperature peaks at the edges where the speed of the flow is smaller. The effect of convection is then to move the region of heated fluid downstream, while the profile is progressively smoothed out by the diffusion in the y -direction contributed by the $\partial^2 T / \partial y^2$ term in Eq. (2.1).

The size of the reduced Peclet number controls the balance between convection and diffusion effects in the chan-

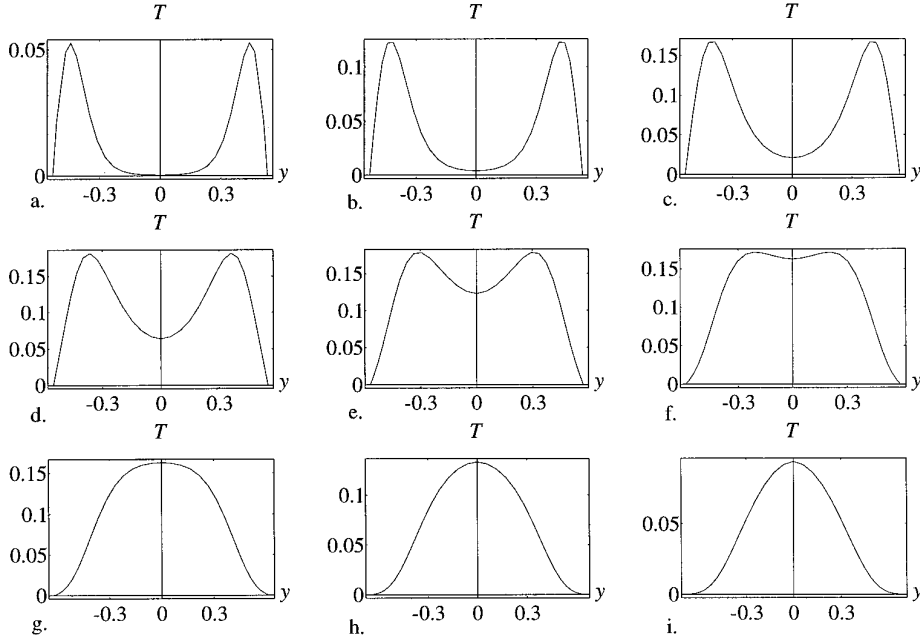


FIG. 5. Cross-sections of $T(x, y, t = 0.005)$ when $Pe = 100$ at $x =$ (a) 0, (b) 0.0731, (c) 0.1459, (d) 0.2182, (e) 0.2896, (f) 0.3601, (g) 0.4295, (h) 0.4977, (i) 0.5647. Calculations were made with $\Delta t = 0.001$ on a grid with 30×30 grid cells in either direction.

nel. This is demonstrated by the results in Figs. 4a–4c, obtained with $Pe = 0.1$, and those obtained with $Pe = 10$ in Figs. 4g–4i. It can be seen that the temperature pulse moves faster and the initial troughing effect is more pronounced the larger the value of Pe . It is perhaps easier to see the shape of the evolving temperature pulse for high values of Pe by plotting cross-sections of the solution at a sequence of stations down the channel at a given time. In Fig. 5 we plot such a sequence of cross-sections when $Pe = 100$. It may be seen that the profile of the pulse gradually transforms from one exhibiting peaks of temperature near the walls to one having a bell shaped profile as the heated fluid emerges into the unheated fluid through the centre of the channel downstream.

5. CONCLUSIONS

In the preceding work an ADI scheme has been developed and successfully applied to model the effect a temperature pulse has upon the temperature distribution within a two-dimensional symmetric channel. The scheme solves a general parabolic differential equation, and has been shown to be unconditionally stable in the case of constant coefficients.

A simple model of flow through a dye laser cell requires the solution of the two-dimensional heat-transport equation within a symmetric converging/diverging channel subject to impulsive heating. The ADI scheme described here was applied to this problem, and the results indicate that

the temperature pulse moves faster through the channel and the initial troughing effect is more pronounced the larger the value of the Peclet number.

APPENDIX A: PROOF OF UNCONDITIONAL STABILITY FOR SECOND ORDER UPWINDING

We apply the method of Section 3.1 and so consider a solution to the difference equation (3.2) of the form

$$T_{i,j}^n = A e^{an\Delta t} e^{\sqrt{-1}\beta i\Delta x} e^{\sqrt{-1}\gamma j\Delta y},$$

in this case, however,

$$\begin{aligned} \nabla_x T_{i,j}^n = & \left[\frac{3}{2} - 2 \cos(\beta\Delta x) + \frac{1}{2} \cos(2\beta\Delta x) \right. \\ & \left. + \sqrt{-1}(2 \sin(\beta\Delta x) - \frac{1}{2} \sin(2\beta\Delta x)) \right] T_{i,j}^n \end{aligned}$$

upon using the second order operation defined by Eq. (3.3), with a similar expression for $\nabla_y T_{i,j}^n$. Defining

$$\begin{aligned} F := & \left(\left[\left[1 - \frac{ra}{2} \delta_x^2 + \frac{pu}{2} \nabla_x \right] \left[1 - \frac{rc}{2} \delta_y^2 + \frac{pv}{2} \nabla_y \right] T_{i,j}^{n+1} \right]^2 \right. \\ & - \left. \left\{ \left[1 + \frac{ra}{2} \delta_x^2 - \frac{pu}{2} \nabla_x \right] \left[1 + \frac{rc}{2} \delta_y^2 - \frac{pv}{2} \nabla_y \right] \right. \right. \\ & \left. \left. + \frac{rb}{4} \delta_{xy} \right\} T_{i,j}^n \right)^2 / |T_{i,j}^n|^2 \end{aligned}$$

as before we have unconditional stability according to von Neumann analysis if and only if $F \geq 0$. Since in the case $u = v = 0$ the scheme again defaults to that of McKee and Mitchell [10] it is sufficient to prove that

$$D(a, b, c, u, v, r, p, \theta, \phi) := F(a, b, c, u, v, r, p, \theta, \phi) - F(a, b, c, 0, 0, r, p, \theta, \phi) \geq 0$$

for all θ, ϕ . After some simplification we obtain

$$\begin{aligned} \frac{1}{8}D &= \left[pv \sin^4\left(\frac{\phi}{2}\right) + pu \sin^4\left(\frac{\theta}{2}\right) \right] \\ &\times \left[1 + 4r^2ac \sin^2\left(\frac{\theta}{2}\right) \sin^2\left(\frac{\phi}{2}\right) - \frac{br}{2} \sin \theta \sin \phi \right] \\ &+ p^2r \sin^2\left(\frac{\theta}{2}\right) \sin^2\left(\frac{\phi}{2}\right) \left[av^2 \left(1 + 3 \sin^2\left(\frac{\phi}{2}\right)\right) \right. \\ &+ cu^2 \left(1 + 3 \sin^2\left(\frac{\theta}{2}\right)\right) - uwb \cos^2\left(\frac{\theta}{2}\right) \cos^2\left(\frac{\phi}{2}\right) \\ &\times \left(1 + 2 \sin^2\left(\frac{\phi}{2}\right)\right) \left(1 + 2 \sin^2\left(\frac{\theta}{2}\right)\right) \left. \right] \\ &+ p^3uv \sin^2\left(\frac{\theta}{2}\right) \sin^2\left(\frac{\phi}{2}\right) \left[u \sin^2\left(\frac{\phi}{2}\right) \right. \\ &\times \left(1 + 3 \sin^2\left(\frac{\theta}{2}\right)\right) + v \sin^2\left(\frac{\theta}{2}\right) \left(1 + 3 \sin^2\left(\frac{\phi}{2}\right)\right) \left. \right] \\ &+ 4rp \sin^2\left(\frac{\theta}{2}\right) \sin^2\left(\frac{\phi}{2}\right) \left[arv \sin^2\left(\frac{\phi}{2}\right) \right. \\ &+ cru \sin^2\left(\frac{\theta}{2}\right) + puw \sin^2\left(\frac{\theta}{2}\right) \sin^2\left(\frac{\phi}{2}\right) \left. \right] \\ &\times \left[c \sin^2\left(\frac{\phi}{2}\right) + a \sin^2\left(\frac{\theta}{2}\right) + \frac{b}{4} \sin \theta \sin \phi \right] \\ &+ 4p^2ruw \sin^4\left(\frac{\theta}{2}\right) \sin^4\left(\frac{\phi}{2}\right) \left[a \sin^2\left(\frac{\theta}{2}\right) \right. \\ &+ c \sin^2\left(\frac{\phi}{2}\right) \left. \right]. \end{aligned}$$

The third and last terms in this expression for D are clearly non-negative while the first and fourth terms are non-negative by Lemmata 2 and 1 respectively. Upon setting $\mu_1 = \sqrt{cu}$, $\mu_2 = \sqrt{av}$ the second term may be written in the quadratic form

$$A\mu_1^2 + B\mu_1\mu_2 + C\mu_2^2,$$

where

$$A = 1 + 3 \sin^2\left(\frac{\theta}{2}\right),$$

$$C = 1 + 3 \sin^2\left(\frac{\phi}{2}\right),$$

$$B = -2 \cos^2\left(\frac{\theta}{2}\right) \cos^2\left(\frac{\phi}{2}\right) \left(1 + 2 \sin^2\left(\frac{\phi}{2}\right)\right) \times \left(1 + 2 \sin^2\left(\frac{\theta}{2}\right)\right),$$

and is non-negative if and only if $A, C \geq 0$ and $4AC - B^2 \geq 0$. Clearly $A, C \geq 0$ and

$$\begin{aligned} 4AC - B^2 &= \left[1 + 2 \sin^2\left(\frac{\phi}{2}\right)\right] \left[1 + 2 \sin^2\left(\frac{\theta}{2}\right)\right] \\ &\times \left[1 - \cos^4\left(\frac{\theta}{2}\right) \left(1 + 2 \sin^2\left(\frac{\theta}{2}\right)\right) \right. \\ &\times \cos^4\left(\frac{\phi}{2}\right) \left(1 + 2 \sin^2\left(\frac{\phi}{2}\right)\right) \left. \right] \\ &+ \sin^2\left(\frac{\theta}{2}\right) \left[1 + 2 \sin^2\left(\frac{\phi}{2}\right)\right] \\ &+ \sin^2\left(\frac{\phi}{2}\right) \left[1 + 2 \sin^2\left(\frac{\theta}{2}\right)\right]. \end{aligned}$$

But

$$0 \leq \cos^4\left(\frac{\psi}{2}\right) \left(1 + 2 \sin^2\left(\frac{\psi}{2}\right)\right) \leq 1$$

for all real ψ so the term inside the square bracket in the above expression for $4AC - B^2$ is non-negative and therefore $4AC - B^2 \geq 0$ and $D \geq 0$ for all θ, ϕ .

ACKNOWLEDGMENTS

DPW acknowledges the financial support of British Nuclear Fuels Ltd. via a studentship. All three authors are grateful to the referees for their constructive comments.

REFERENCES

1. V. B. Andreev, *U.S.S.R. Comput. Math. Math. Phys.* **7**, 92 (1967).
2. R. M. Beam and R. F. Warming, *SIAM J. Sci. Stat. Comput.* **1**(1), 131 (1980).

3. I. J. D. Craig and A. D. Sneyd, *Comput. Math. Appl.* **16**(4), 341 (1988).
4. I. J. D. Craig and A. D. Sneyd, *Comput. Math. Appl.* **20**(3), 53 (1990).
5. J. Douglas and J. E. Gunn, *Numer. Math.* **6**, 428 (1964).
6. F. J. Duarte and L. W. Hillman, *Dye Laser Principles* (Academic Press, San Diego, 1990).
7. C. A. J. Fletcher, *Computational Techniques For Fluid Dynamics*, Vol. 2 (Springer-Verlag, Berlin/New York, 1988).
8. B. Heron, *Applic. Anal.* **12**, 197 (1981).
9. P. D. Lax and R. D. Richtmyer, *Comm. Pure Appl. Math.* **9**, 267 (1956).
10. S. McKee and A. R. Mitchell, *Comput. J.* **13**, 81 (1970).
11. D. W. Peaceman and H. H. Rachford, *J. SIAM* **3**, 28 (1955).
12. A. A. Samarskii, *Zh. Vychisl. Mat. Mat. Fiz.* **2**(5), 787 (1964).
13. F. P. Schäfer, *Dye Lasers, Topics in Applied Physics*, Volume 1 (Springer-Verlag, Berlin, 1974).
14. M. Vinokur, *J. Comput. Phys.* **50**, 215 (1983).
15. R. F. Warming and R. M. Beam, *BIT* **19**, 395 (1979).